Seismic Activity at the Tarbela Dam Site and Surrounding Region[1,2]

L. SEEBER, J. ARMBRUSTER and S. FARHATULLAH

Abstract: The earthquake activity associated with the major faults of the Himalayan front in the Hazara arc region, including Tarbela dam, is discussed in terms of the active tectonic structure of this front. Moreover, the earthquake potential at the Tarbela site arising from the Indus fault system is evaluated by extrapolating the earthquake magnitude distribution.

The active tectonics associated with plate convergence in the Hazara arc region of the Western Himalayas has been modeled primarily by using earthquake data from the seismic network centered at Tarbela. The near-surface structural trends in Hazara are distinct and separated from the trends along the Himalayan front in Kashmir by the Hazara-Kashmir syntaxis. In contrast, the deeper structures which are active within the basement in Hazara are continuous with, and linear extensions of the northwest trending structures of the Himalayas in Kashmir. Thus, the arcuate structures in Hazara are only thin-skin. A major detachment fault decouples the sedimentary and metasedimentary layer of the thrust-and-fold belt from the underlying basement. The relative motion on the detachment obtained from seismic data is consistent with the southward vergence of the structures in this belt.

Three families of active faults are recognized as potential sources of destructive earthquakes in the Hazara arc region and, in particular, at the Tarbela dam site: the basement faults; the detachment fault; and faults within the sedimentary layers. Available intensity and instrumental data indicate that the Himalayan Basement Thrust and associated transverse or tear faults are the locus of most of the epicenters, however, the largest ($M \geqq 8$) and most damaging earthquakes occur on the Himalayan Detachment. The Hazara arc is included in the tectonic province of the Himalayan front, thus the Basement Thrust and the Detachment are identified with corresponding structures in Hazara, and the earthquake potential is estimated accordingly.

A layer of thick Infracambrian salt is associated with the Detachment in the Hazara arc region. The low-strength properties of this layer may cause the slip on this portion of the Detachment to occur aseismically. In this case, major Detachment earthquakes analogous to those known from the central section the Himilayan front would not be expected in the Hazara region.

The sedimentary layer in the Tarbela network region of the Hazara arc is mostly aseismic except for the Tarbela seismic zone (TSZ), centered near the Tarbela dam site. This sharply defined volume of seismicity is probably associated with anomalous rock properties rather than an isolated zone of crustal deformation. Thus, the faults active within the TSZ may slip aseismically in the sedimentary layer outside the TSZ.

The maximum credible earthquake in the TSZ is assigned a magnitude 6,5, a maximum surface acceleration of 0.5g, and is associated with the surface rupture of one of the faults in the Indus Valley at the Tarbela site. From a quantitative study of earthquake-magnitude distribution a repetition time of 1,200 years is obtained for the maximum credible event. This implies a probability of 1/24 that this event will occur during a 50-year life-time of the dam. The maximum probable earthquake at the Tarbela site in 50 years is a $M = 5.5$ event. The rate of seismicity along the Indus fault system at the Tarbela site is 50 times higher than the average seismicity for the Hazara arc region. However, the level of seismicity on the TSZ is well below the seismicity associated with some of the other seismic zones within the Hazara arc. Most prominent among these is the IKSZ.

TECTONIC SETTING

1. The Hazara Arc

The active structures associated with continental convergence in the extreme northwestern portion of the Himalayan front (Figures 1, 2 and 3) have been inferred primarily on the basis of seismic data from the Tarbela network in northern Pakistan (Figure 4) (Armbruster *et al.*, 1978; Seeber and Jacob, 1978; Seeber and Armbruster, 1979). The major basement faults are clearly indicated by the seismicity and have an obvious topographic expression, but these faults do not show any direct correlation with surface structures. A decoupled sedimentary and metasedimentary wedge shaped into an arcuate thrust-and-fold belt is the main surface feature of the Hazara arc and masks the underlying basement faults (Figures 4, 5 and 6).

In Figure 6, hypocenters in the lower crust clearly delineate two parallel seismic zones about 150 km long: the Indus Kohistan seismic zone (IKSZ) and the Hazara

[1] Lamont-Doherty Geological Observatory Contribution Number 2859.
[2] The views expressed here are solely the views of the authors and not necessarily the views of L-DGO, WAPDA or TAMS.

Proc. Intern. Commit. Geodynamics, Grp. 6, Mtg. Peshawar, Nov. 23-29, 1979: Spec. Issue, Geol. Bull. Univ. Peshawar, Vol. 13, 1980.

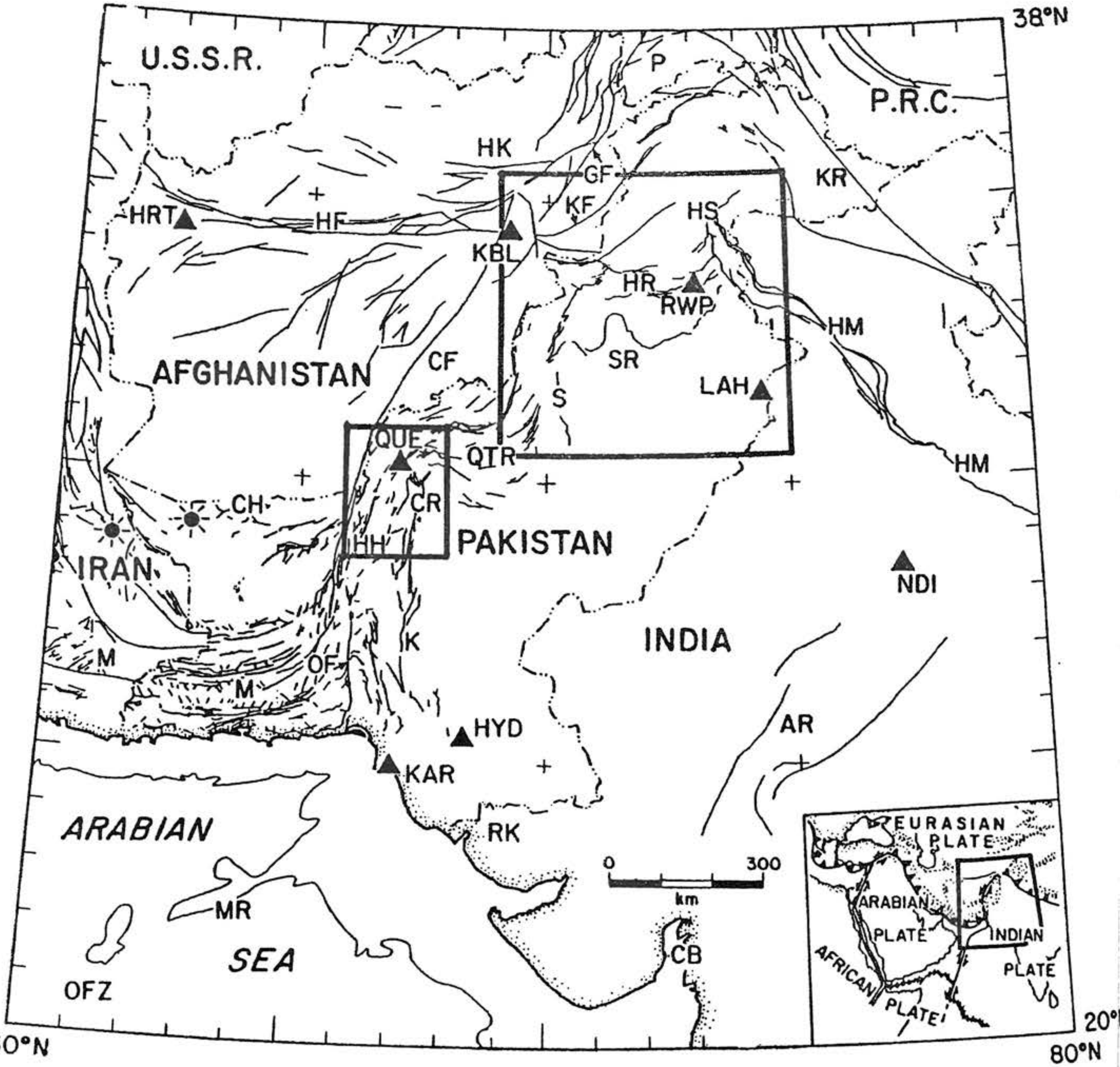

Fig. 1. International boundaries and major surface faults in Pakistan and surrounding areas (from Quittmeyer and Jacob, 1979). The area covered by the networks established by L-DGO in collaboration with Pakistan government agencies are boxed in. The Tarbela and Chashma networks (Figure 4), are in the larger box. The Quetta network is in the smaller box. The filled circles in Iran and Pakistan represent centers of Quaternary volcanism. Geographic features indicated areas as follows: AR =Aravalli range, CH = Cambay basin, CF = Chaman fault, CH = Chagai hills, CR = Central Brahui range, GF = Gardez fault, HR = Hazara range, HF = Herat fault, HH = Harboi hills HK = Hindu Kush region, HM = Himalayas, HS = Hazara-Kashmir syntaxis, K = Kirthar range proper, KF = Kunar fault, KR = Karakorum region, M= Makran region, MR = Murray ridge, OF = Ornach-Nal fault, OFZ = Owen fracture zone, P = Pamirs, QTR = Quetta transverse ranges, RK = Rann of Kutch, S = Sulaiman range, and SR = Salt range. Several cities are indicated by filled triangles: HRT = Herat, HYD = Hyderabad, KAR = Karachi, KBL = Kabul, LAH = Lahore, NDI = New Delhi, QUE = Quetta, RWP = Rawalpindi. The inset in the lower right hand corner shows the plate tectonic setting of the region studied.

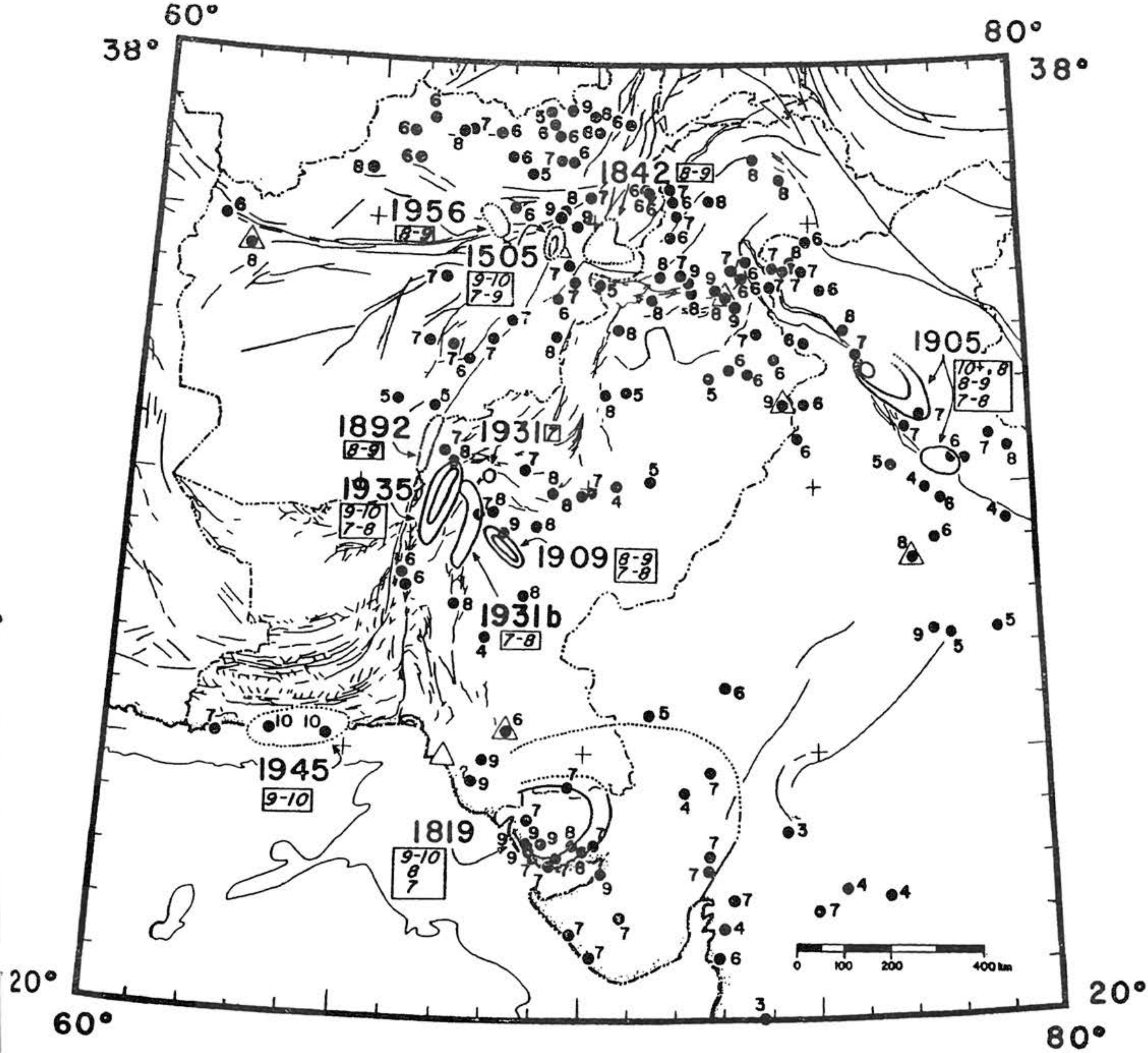

Fig. 2. Map of maximum documented intensity (Modified Mercalli Scale) from 25 A.D. to 1972. Mapped portions of the U.S.S.R., China and Iran are not considered. Isoseismal lines (dotted where inferred) are plotted for some of the larger events. The year of occurrence for each such large event is indicated. The intensity value associated with a given isoseismal line is indicated in the box near each date. The first value given is for the innermost isoseismal line, etc., (from Quittmeyer and Jacob, 1979).

Lower seismic zone (HLSZ). Focal mechanism solutions indicate that the IKSZ is a thrust fault dipping to the northeast whereas the HLSZ is a vertical, right-lateral strike-slip fault (Figure 7). Both these faults strike northwest, parallel to the trend of the Himalayan front east of the Hazara-Kashmir syntaxis (Figures 3 and 4); they are interpreted as the northwestern extension of the main basement faults along this section of the Himalayas (Armbruster *et al.,* 1978).

In the model shown in Figure 7 the sediment-basement interface is a major tectonic boundary, a quasi-horizontal surface of detachment separating different regimes of deformation. The basement is characterized by brittle behaviour while the "sedimentary wedge", or decollement, is characterized by ductile behaviour.

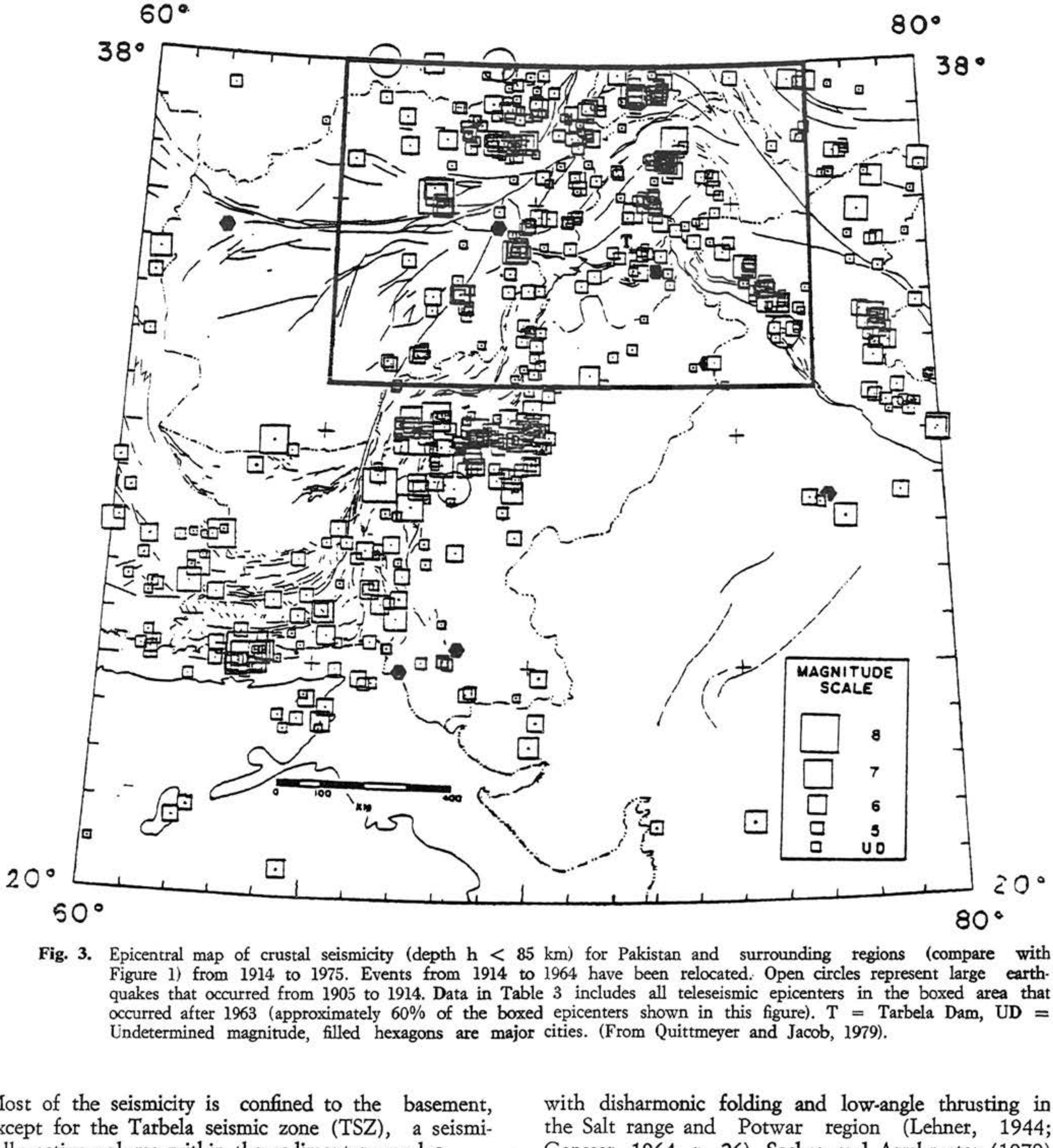

Fig. 3. Epicentral map of crustal seismicity (depth h < 85 km) for Pakistan and surrounding regions (compare with Figure 1) from 1914 to 1975. Events from 1914 to 1964 have been relocated. Open circles represent large earthquakes that occurred from 1905 to 1914. Data in Table 3 includes all teleseismic epicenters in the boxed area that occurred after 1963 (approximately 60% of the boxed epicenters shown in this figure). T = Tarbela Dam, UD = Undetermined magnitude, filled hexagons are major cities. (From Quittmeyer and Jacob, 1979).

Most of the seismicity is confined to the basement, except for the Tarbela seismic zone (TSZ), a seismically active volume within the sedimentary wedge.

The detachment extends as far south as the Salt Range and accommodates shortening of the folded sedimentary wedge as well as southward motion of this wedge relatively to the basement (Figures 4 and 7). The Infracambrian salt formation which outcrops at the base of the south-facing cliff of the Salt range monocline (Gansser, 1964, p. 26) has been associated with disharmonic folding and low-angle thrusting in the Salt range and Potwar region (Lehner, 1944; Gansser, 1964, p. 26). Seeber and Armbruster (1979) suggest a close association between the Infracambrian salt and the detachment in much of the Hazara arc region. The gentle northward dip of the detachment in the Potwar between the Salt range and the Hazara thrust is well determined by oil exploration data (M. Hussain, AMOCO, personal communication). North of the Hazara thrust, the model shown in Figure 7 is based entirely on seismic data.

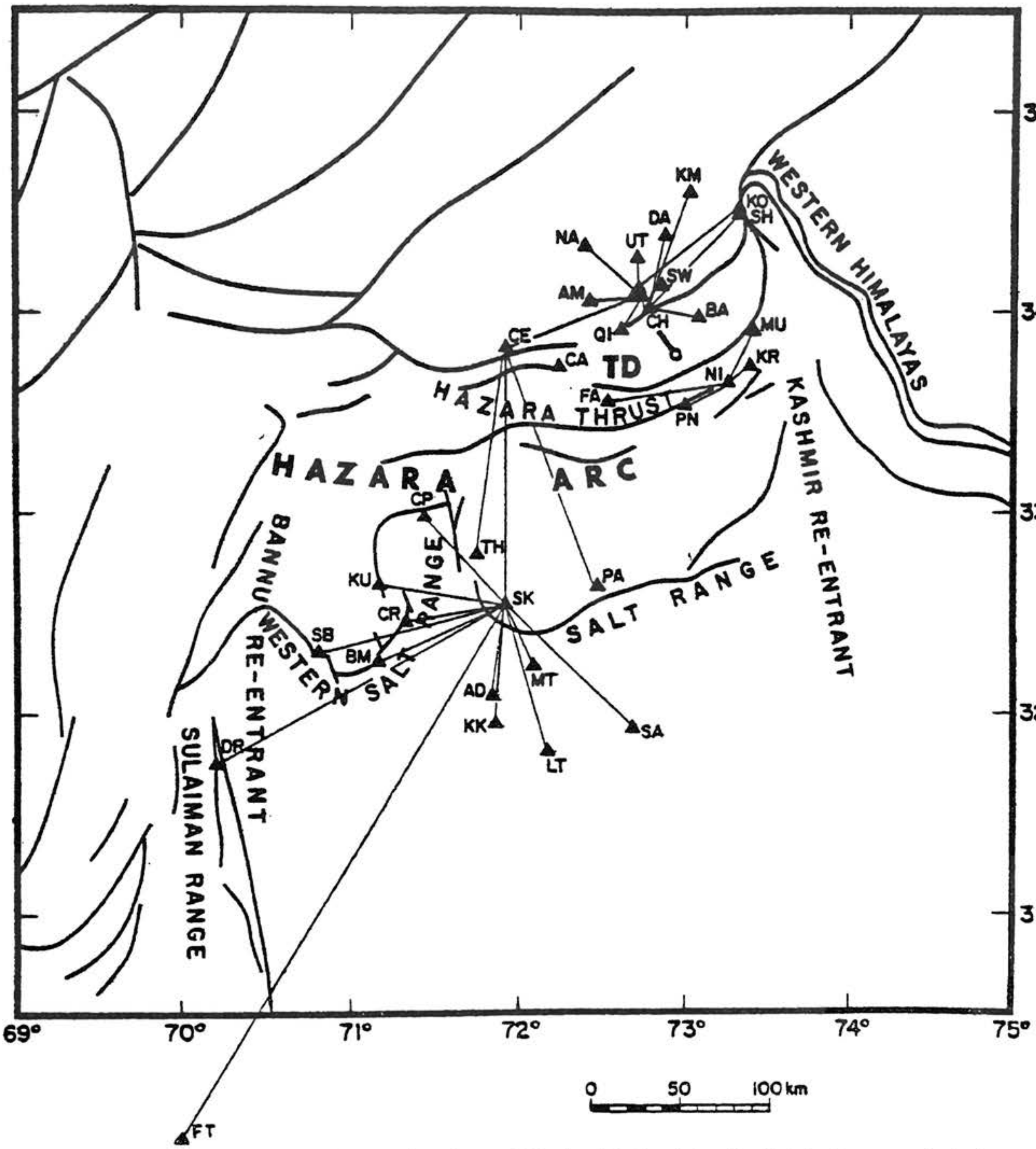

Fig. 4. Station distribution (triangles) and telemetry-links (straight lines) for the Tarbela dam network in the northeast and for the Chashma power plant network in the southwest portions of map. Central recording was at Tarbela dam (T.D.), for both networks up to June 1977. After that, the Chashma network has been operated by the PAEC and central recording shifted to Nilore (Ni). Structural trends are indicated for orientation and may be compared to Figure 1. The Farooquia Quarry site is identified by a small circle and it is linked to the central recording station (TA) through the relay station CH.

II. Analogy to the Central Himalayas

The convergence between the Indian and the Eurasian plates is partially accommodated at the Himalayan front by thrusting, and a zone of thickened crust is formed along this fault (Gansser, 1964, plate II; LeFort, 1975; Molnar *et al.,* 1977). The stratigraphic throw on the Himalayan thrust is very large (Bordet *et al.,* 1971) and may include the entire thickness of the crust, so that subduction (Bailly, 1979) and doubling of the crust may occur (Powell and Conaghan, 1973; Toksoz and Bird, 1977).

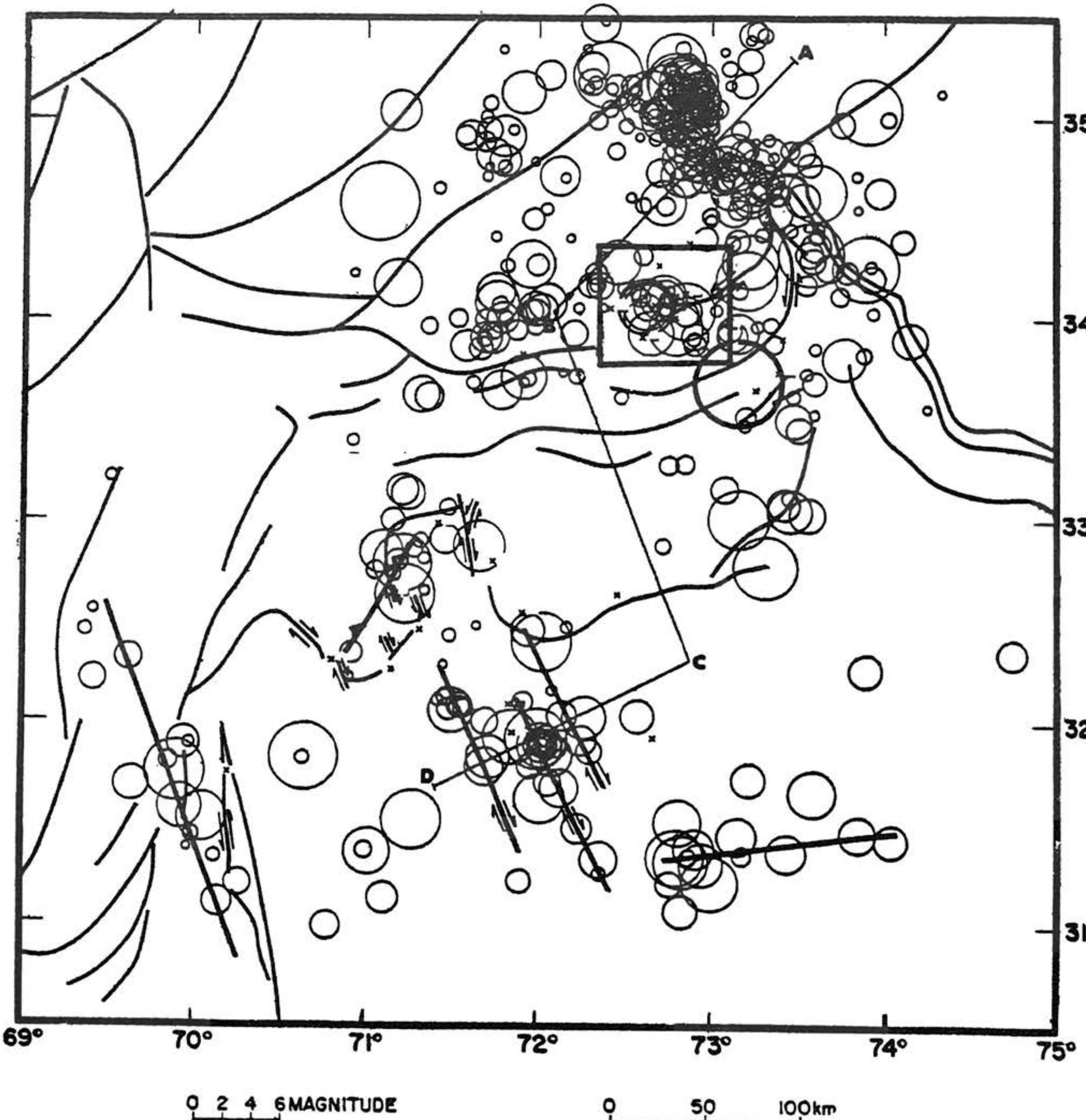

Fig. 5. Six months of epicentral data from the Tarbela and the Chashma networks (from May to November, 1976 from the Chashma network; from February to August, 1976 from the Tarbela network). Compare to Figure 4 for location names (all depths; compare to Figure 6). The epicenter of the February 14, 1977 Rawalpindi earthquake is also shown (largest circle in the figure). Only earthquakes of mag. 0.5 or greater are plotted to obtain a picture of the seismicity within the area of the network unbiased by station sensitivity. This short sample is comparable to the longer term seismicity (see Seeber and Jacob, 1977; Figure 2). The main structural features known from geologic work are shown in thinner lines; major fault zones inferred from the seismicity in the southern part of the Hazara arc are indicated in thicker lines. (From Seeber and Armbruster, 1979).

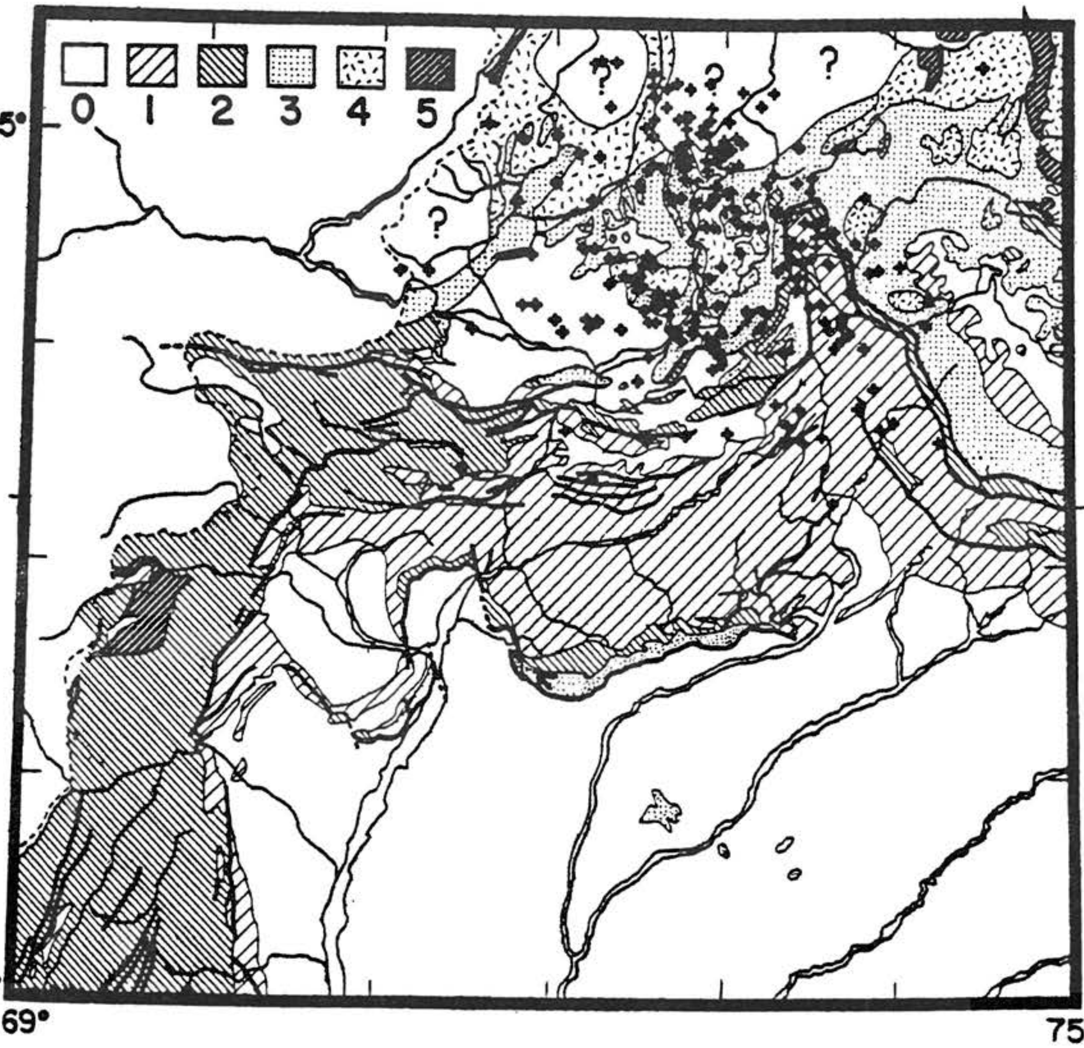

Fig. 6. Geological sketch map of the Hazara arc and surrounding areas in northern Pakistan (modified from Bakr and Jackson (1964). No geologic information is shown for areas in Afghanistan. 0) post-Siwalik basins; 1) Siwalik and Murree (post-collisional); 2) lower Tertiary (pre-collisional) and Mesozoic; 3) Paleozoic and Precambrian; 4) granites (Tertiary ?); 5) ophiolites. Thick lines are faults, mostly northward dipping thrusts. Epicenters with well-determined hypocentral depths greater than 40 km are indicated by crosses (3 years of data). Compare with Figure 4 for location names. Note the two parallel seismic syntaxis. The narrower zone to the southwest is the Hazara Lower seismic zone (HLSZ) and the wider one to the northeast is the Indus Kohistan seismic zone (IKSZ). Compare with Figure 7. (From Seeber and Jacob, 1977).

Seeber *et al.* (1979) suggest that the Himalayan thrust consists of two distinct portions which are contiguous in the dip direction (Figure 8). The shallow portion dips northward very gently and separates the Archean basement of the Indian shield, below, from a wedge of sediments and metasediments, above. This portion is referred to as the Detachment. The Detachment merges down-dip into a steeper portion of the Himalayan thrust that juxtaposes basement rocks of the Indian shield in the foot-wall with similar rocks in the hanging wall. This deeper portion of the Himalayan thrust is referred to as the Basement Thrust.

The transition between the Detachment and the Basement Thrust separates a region of single crustal thickness in the south from one of double crustal thickness in the north. A spectacular surface expression of this transition is the pronounced topographic step between the High and the Lesser Himalayas. This topographic step and the epicenters that can be correlated with the Basement Thrust are found to follow closely the same small circle delineating an arc about 1700 km long. Both the seismicity and the topographic step deviate together from the small circle near the western end of the Himalayan front, in Kashmir, and near the eastern end in Assam (Seeber *et al.*, 1980).

The Main Central Thrust (MCT) and the Main Boundary Fault (MBF) are two among other imbricate offshoots from the Basement Thrust and the Detach-

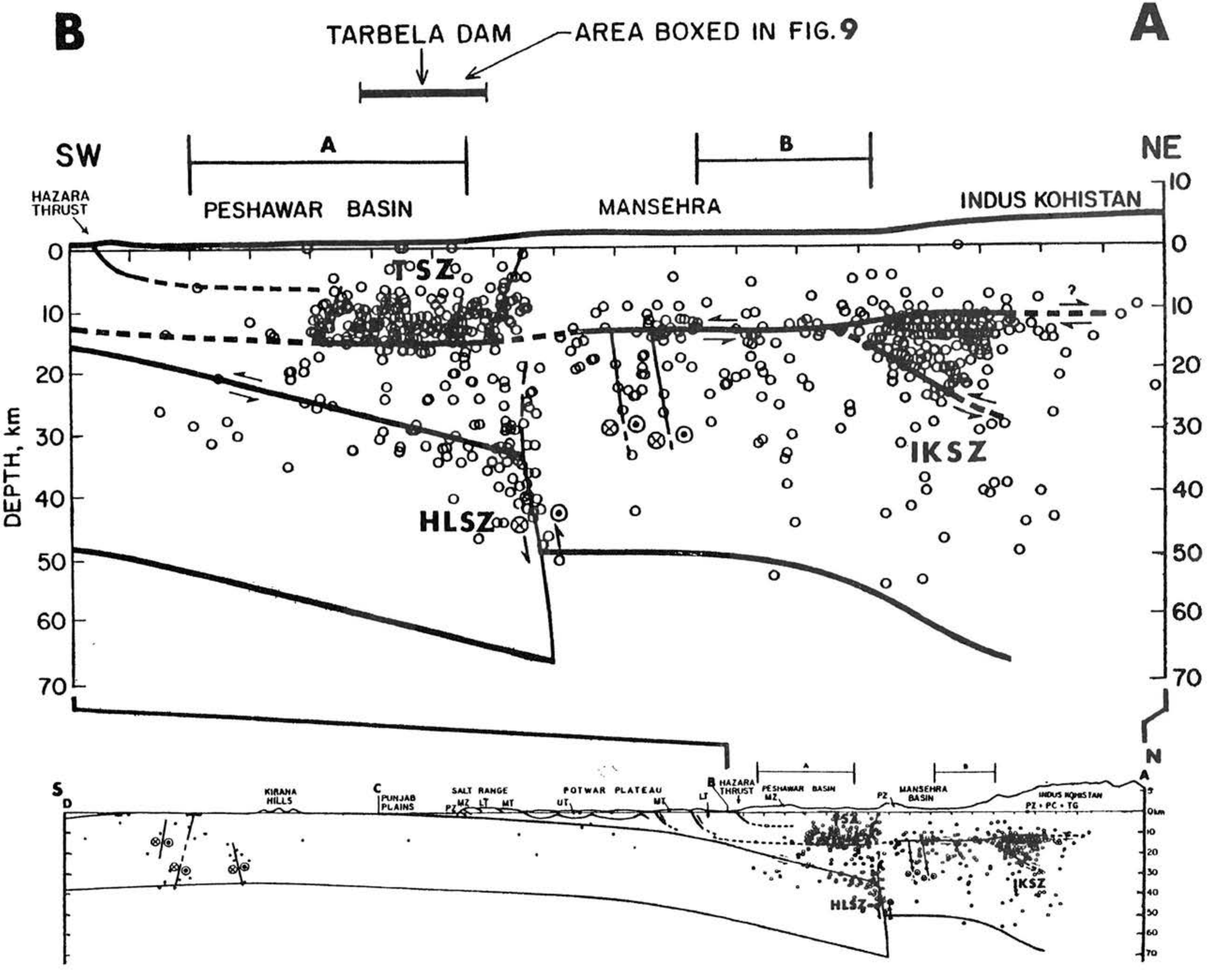
B
TARBELA DAM
AREA BOXED IN FIG. 9
A
SW
NE
HAZARA THRUST
PESHAWAR BASIN
MANSEHRA
INDUS KOHISTAN
TSZ
HLSZ
IKSZ
DEPTH, km
S
D
C
N
KIRANA HILLS
PUNJAB PLAINS
SALT RANGE
POTWAR PLATEAU
MANSEHRA BASIN

Fig. 7

ment, respectively (Figure 8). Although both the MCT and the MBT are probably active faults, their significance in the present tectonic regime is secondary.

The principal elements of the structures related to the ongoing convergence in the Central Himalayas and in the Hazara arc are quite similar (compare Figures 7 and 8). This is in accordance with the hypothesis of Armbruster *et al.* (1978) that the western part of the Hazara arc is part of the Himalayan front. The IKSZ in the Hazara arc can be readily identified with the Basement Thrust of the Himalayas. In both sections, the main thrust merges upward into the quasi-horizontal Detachment that approaches the surface south of the molasse basin, a few hundred kilometers toward the foreland from the Basement Thrust.

The structurally complex western terminus of the Himalayan front is characterized by a few prominent features which are anomalous. Of interest here are: the HLSZ; the broad belt of folding in the Potwar; the Salt Range; the extension of the Detachment north of the IKSZ (Figure 7); and a second active branch of the Basement Thrust, parallel to and northeast of the IKSZ, which may extend through the Gilgit region (Figure 3; Seeber *et al.*, 1980). These features are briefly discussed below.

Assuming rigid plate tectonics, the convergence of the Indian and Eurasian plates in the Hazara region is approximately northward at about 3.7 cm/year (Armbruster *et al.*, 1978). Both the IKSZ and the HLSZ account for some of this convergence, although a large fraction of the convergence may occur north of the Himalayas (Molnar and Tapponnier, 1975). Fault plane solutions from both teleseismic (Pennington, 1979A) and network data (Armbruster *et al.*, 1978) indicate that the thrusting on the IKSZ and the right-lateral strike-slip on the HLSZ are associated with slip toward the northeast and towards the northwest, respectively. The resulting convergence must lie in between these directions as it is predicted by rigid plate tectonics.

Thus, the oblique convergence at the western terminus of the Himalayas is accomplished by two parallel faults with pure dip-slip (IKSZ) and pure strike-slip (HLSZ), respectively. This pattern has been observed in oblique convergence zones elsewhere (Fitch, 1972). Tear faults perpendicular to the basement thrusting are common in the Hazara arc region (Seeber *et al.*, 1980). The offsets associated with these tear faults would tend to constrict the convergence on the IKSZ to be pure thrusting.

In the central section of the Himalayan front the thrusted and folded region of the molasse basin extends only a few tens of kilometers south of the MBF (Figure 8; Gansser, 1964, plate II). In the Hazara arc, the folded molasse of the Potwar extends about 100 km south of the Hazara thrust, the equivalent of the MBF in this region. Moreover, this folding terminates in the Salt range, a structure not found elsewhere along the Himalayan front. Both these features suggest an unusually low coupling on the Detachment in the Hazara arc. The thick Infracambrian salt layer associated with the Detachment in this area (Seeber and Armbruster, 1979A) is expected to play a major role.

Similarly, the peculiar interaction between the IKSZ and the Detachment (Figure 7) forming a structure reminiscent of flake tectonics in the eastern Alps (Oxburg, 1972; Seeber and Jacob, 1977), may also be caused by the unusually weak coupling on the Detachment.

Very little is known about the postulated branch of the Basement Thrust associated with the seismic activity in the Gilgit region. This seismicity falls on the small circle fitted to the central portion of the Basement Thrust, while the branch of the Basement Thrust associated with the Panjal range and the IKSZ clearly deviates from this circle (Seeber *et al.*, 1979).

SEISMIC POTENTIAL IN THE TARBELA DAM AREA OF THE HAZARA ARC

Three distinct families of active faults are associated with a seismic potenial of concern to the Tarbela dam site and to the surrounding area of the Hazara arc: the Basement Thrust and other basement faults, the Detachment, and faults within the sedimentary wedge.

Fig. 7. The active tectonic structure beneath the seismic network as tentatively deduced from the seismicity. The most reliable hypocentral data from a strip along this section is also plotted; the section is located in Figure 5. Note that while the seismicity level is fairly represented in Figure 5, in this section the seismicity is biased in favour of the TSZ, near the center of the network, since no magnitude cut-off is applied. The sense of movement on the faults in the portion A-B of the section is known from composite fault-plane solutions: ⊗ = motion away from viewer; ⊙ = motion toward viewer; UT, MT, LT = upper, middle, lower Tertiary; MZ = Mesozoic; PZ = Paleozoic; PC = Precambrian; TG = Tertiary granite; HLSZ = Hazara Lower seismic zone; IKSZ = Indus-Kohistan seismic zone; TSZ = Tarbela seismic zone. The detachment, the quasi-horizontal fault that extends from the base of the Salt range to the IKSZ and beyond, is active even where seismicity is presently absent. On these portions of the Detachment slip may occur either aseismically or by rare large earthquakes (compare with Figure 8). The distribution of seismicity in the Salt Range and the Potwar Plateau is somewhat distorted by the linear projection along a curved structure; most of the seismicity occurs along the Salt Range and not in the Potwar Plateau (see Figure 5) (From Seeber *et al.*, 1979).

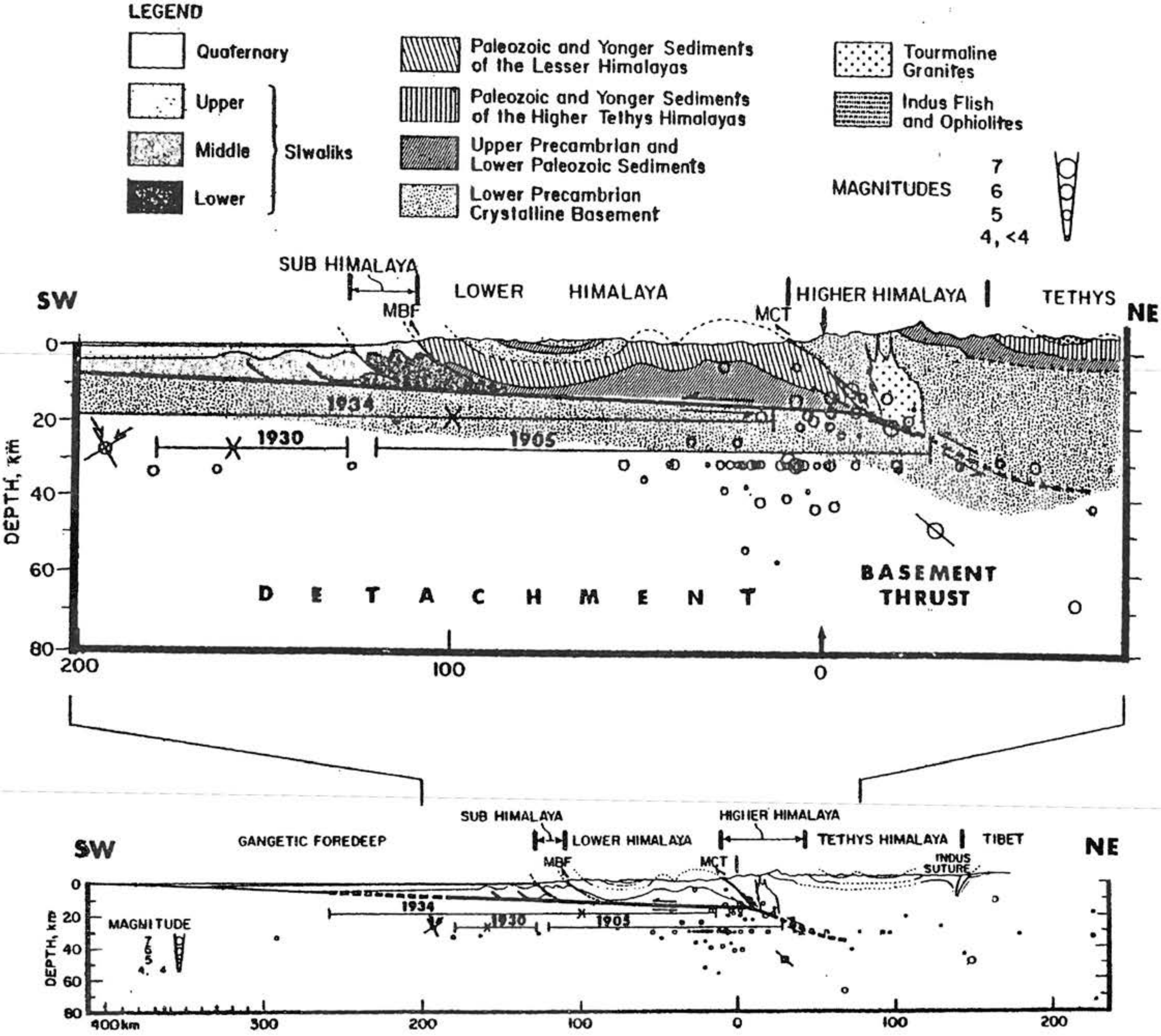

Fig. 8. Section of the geology and seismicity in the central Himalayas (from Seeber *et al.*, 1979). NOAA (1963-1975) hypocenters are projected along the Himalayan arc from 78E to 83E (approximately) on a plate perpendicular to the arc. Fault-plane solutions for some of the earthquakes in this set are indicated: the segments drawn across the hypocenter represent one of the two possible planes of slip as viewed in the section. All the slip vectors on the northward-dipping plane agree with the sense of motion indicated on the basement thrust except for the earthquake 200 km south of the basement thrust which is associated with normal faulting. The concentration of hypocenters at 33 km depth is not real: this depth is assigned to all earthquakes for which an independent depth determination is not available. The epicenters and the extent of intensity VIII (Mercalli I-X scale) associated with the 1905 Kangra M = 8, 1930 Dhubri M = 7.1 and the 1934 Bihar M = 8.4 events are shown by large crosses and horizontal lines, respectively. Note that the major events in this century seem to be associated with rupture of the Detachment while the moderate size earthquakes in the last decade are concentrated at the transition zone between the Detachment and the Basement Thrust (see text). Surface geology is from Gansser (1964; plate II, section A). Below sea level structures are somewhat modified to fit the model obtained from the seismicity.

Most of the information pertinent to the discussion of the earthquake hazard from the Basement Thrust and the Detachment in Hazara is derived from the characteristic behaviour of these structures along the Himalayan front. However, seismic zones within the sedimentary wedge similar to the TSZ have not yet been recognized elsewhere along the Himalayan front. Thus, the earthquake potential from the TSZ is evaluated per se from the Tarbela network data and from teleseismic data.

I. Basement Fault and Detachment

Seeber *et al.* (1979) indicate that the two well documented great earthquakes in the central section of the Himalayan front, the 1905 Kangra (M 8.0) and the 1934 Bihar (M 8.4) earthquakes, are associated with ruptures on the Detachment, while most of the moderate to major earthquakes ($M \leq 7.5$) are associated with the Basement Thrust (Figure 8). (We follow Quittmeyer *et al.* (1979) in our use of qualifiers for earthquake size: Moderate, $6 \leq M < 7$; Major, $7 \leq M < 7.8$; Great, $M \geq 7.8$). Typically ruptures occur over vast portions of the Detachment in a single event and generate great earthquakes. In the periods between these events the Detachment appears to be aseismic. On the other hand, the Basement Thrust is associated with relatively continuous seismicity and with a reduced upper-magnitude limit. Only the portion of the Basement Thrust adjacent to the Detachment appears to be seismically active (Figure 7). Slip may occur aseismically because of shear-heating (LeFort, 1975) and/or from availability of water on deeper portions of the Basement Thrust. A similar pattern of seismicity is observed at oceanic subduction zones (Isacks and Barazangi. 1977; Hasegawa *et al.*, 1977; Davies and House, 1979).

The contrasting seismic behaviour of the Detachment and the Basement Thrust has profound implications regarding the seismic hazard along the Himalayan front. While a relatively short sample of the seismicity (for example the hypocenters in Figure 7) would suggest that the hazard is highest along the Basement Thrust, a longer sample of seismicity viewed in the framework suggested by Seeber *et al.* (1979) and Seeber *et al.* (1980) indicates that the hazard is highest in the tectonic province of the Detachment which extends from the Basement Thrust southward to and including the Gangetic foredeep.

In the relatively short data sample available from the Tarbela network, most of the seismicity is associated with the IKSZ, or the Basement Thrust, and the Detachment is almost aseismic. In a first estimate of the seismic hazard, the conclusions concerning the Himalayan front must also be valid for the Tarbela region, and great earthquakes should be expected on the Detachment and not on the IKSZ. At any location between the Salt range and the IKSZ the depth to the Detachment is from a few kilometers to a maximum of 17 km. A similar range of depth can be assigned to the Detachment in the area of the 1934 Bihar event (Mathur and Evans, 1964), thus similar maximum intensities can be expected in Bihar and in the Hazara arc region.

The data suggest a continuous detachment along the entire length of the Himalayan front including the Hazara arc, but the mode of slip on the Detachment may be discontinuous along this front. While in the Hazara arc the Detachment is associated with the thick Infracambrian salt layer, oil exploration data from the Sub-Himalayas and the Gangetic foredeep indicate that a salt layer at the sediment-basement boundary is not present at least between and including the mezoseismal areas of the 1905 and 1934 events (Mathur and Evans, 1964).

Evaporites deform more readily than any other consolidated sediments. Their strength decreases rapidly with raising temperature and, therefore, with increasing depth of burial. At 100°C, or at a depth of about 3 km for a normal geothermal gradiant, salt (halite) is expected to behave like butter (Borchert and Muir, 1964, p. 279). Thus, the Detachment in the Hazara arc region which is associated with the Infracambrian salt, may move primarily by aseismic slip rather than earthquakes.

Whether slip on the Detachment in the Hazara arc occurs aseismically or in major earthquakes is crucial to seismic hazard evaluation in this area. This question will be resolved only when direct evidence for aseismic slip becomes available from geodetic or other measurements.

The IKSZ, 70 km northeast of the Tarbela site is part of the Himalayan Basement Thrust that stretches for 2,500 km along the Himalayan front. The history of the seismicity along this front suggests that the upper magnitude limit for earthquakes on the Basement Thrust is relatively low considering the length of this fault. The effects of the 1974 Pattan ($M_b = 6.0$) earthquake (Ambraseys *et al.*, 1975), which occurred at the northwestern end of the IKSZ, may not be unusual for the larger earthquakes on this seismic zone. Thus, the vibration potential at the Tarbela dam site from the maximum credible earthquakes on the IKSZ is relatively low.

However, large earthquakes on the IKSZ or on other seismic zones upstream of the Tarbela reservoir may induce slides involving a large volume of unconsolidated sediments, rock and ice that may temporarily block the river flow. A catastrophic flood may ensue when these natural dams burst (Ambraseys *et al.*, 1975). The many recent terraces and lake deposits in the Indus

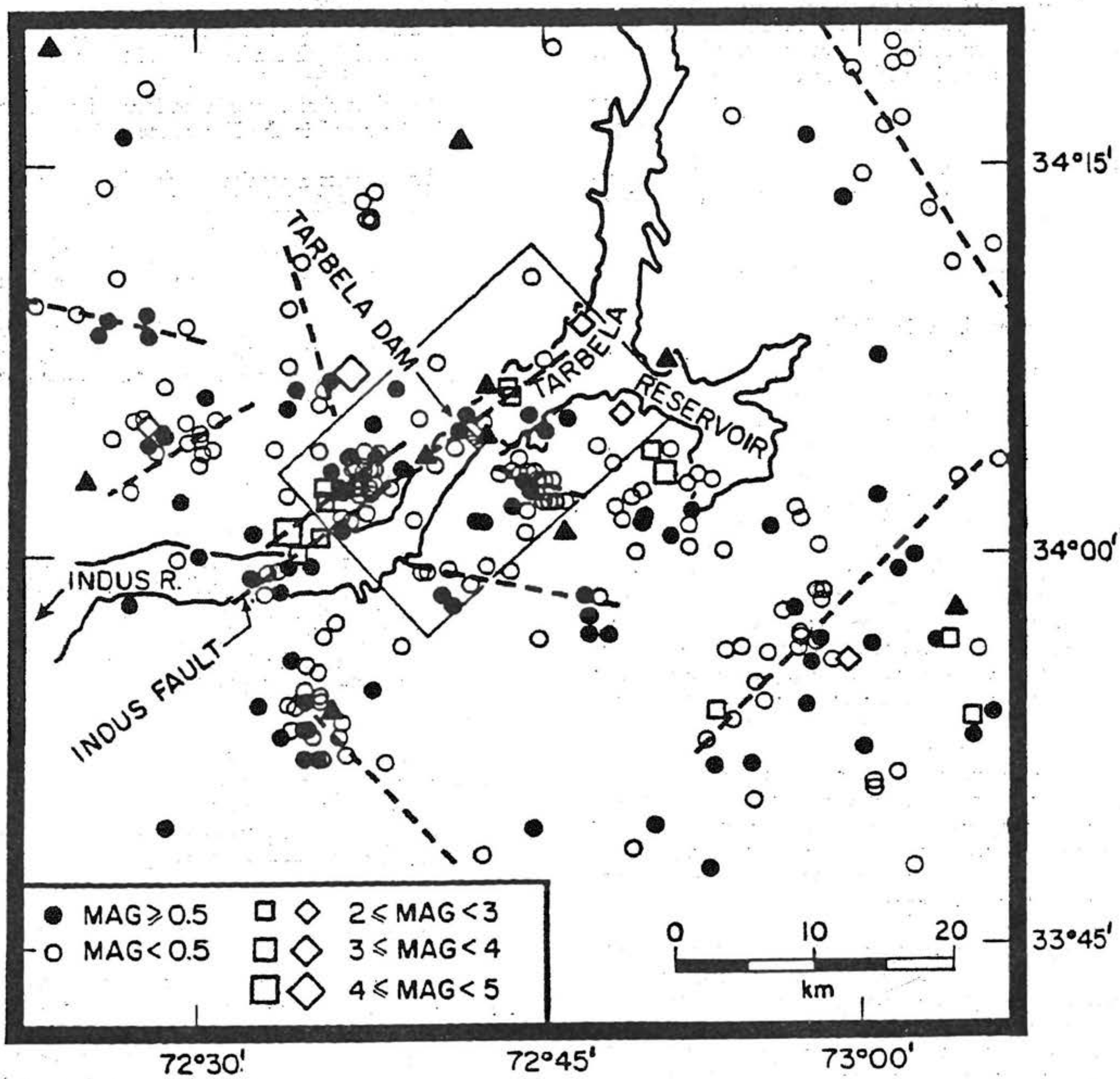

Fig. 9. Seismicity in the Tarbela area detected by the local network (solid triangles; other stations fall outside the map). Circles are for earthquakes that occurred between August 1973 to August 1976. These earthquakes are located by computer and only the ones between the depth of 15 and 20 km are plotted. Epicentral maps of restricted depth-ranges display more clearly epicenter alignments because different patterns of faulting are found at different depths (see Figure 7).. Dashed lines are strike of fault planes, mostly steeply dipping, as determined by composite fault-plane solutions superimposed on the associated seismic patterns (see Armbruster *et al.*, 1978). Note the general agreement between these lines and the epicenter alignments. Squares (hypocentral depth $0 < h \leq 20$ km) and diamonds ($20 < h \leq 30$) are epicenters for more recent earthquakes (August 1976 to January 1978) with magnitude $M \geq 2$. These epicenters have been graphically deter-mined by the WAPDA seismologists at the Tarbela site. None of these earthquakes occur at depth $h < 10$ km. The shallower ($10 < h \leq 20$) of these recent events are concentrated along the Indus fault system (7 out of 12 epicenters) conforming to the previously noted distribution of the seismicity in the Tarbela area (Seeber *et al.*, 1974). The area of this figure is boxed in Figure 5.

river gorge upstream of Tarbela and the large, non-glacial exotic boulders in the river terraces at Tarbela and as far south as the Potwar (Wadia, 1961, p. 410) are the evidence of these catastrophic floods. The last of these events in the Indus basin occurred in 1841 (TAMS, 1964). The spillway capacity (1.5×10^6 cusecs) and the free-board/width of the Tarbela embankment crest are designed to withstand the impact of the flood following the collapse of a natural dam. Since the damming of a major river is not likely to escape notice and the ensuing flood can be anticipated, the Tarbela reservoir can be used as a buffer to prevent a disaster further downstream.

Very little data are available for an estimate of the seismic potential associated with the HLSZ (Figure 7). The seismicity on this deeply buried basement fault is low relative to the seismicity on the IKSZ (compare Figures 5 and 7), although both of these parallel structures can be traced seismically for at least 100 km (Seeber and Armbruster, 1979A). If these two fault zones contribute similarly to the continental convergence at the Himalayan front (see discussion above) a comparable rate of slip would be expected on these two faults. Since the seismicity presently observed on the HLSZ is relatively low, this movement would have to be accomplished either by aseismic slip or by rare large earthquakes. The 25 AD Taxila event (Ambraseys, 1975) could be associated with one of these earthquakes. Thus, the possibility of large earthquakes on the HLSZ cannot at present be ruled out.

II. Seismicity Within the Sedimentary Wedge – The TSZ and the Indus Fault System

A. Tectonics. The decollement, the sedimentary and metasedimentary wedge above the detachment, is characterized by low seismicity except for the Tarbela seismic zone (TSZ). The TSZ is a sharply bounded cluster of hypocenters near the center of the Tarbela network above the HLSZ (Figure 7). The detailed 3-dimensional distribution of hypocenters and composite focal mechanism solutions, indicate that this seismicity is occurring on many steeply-dipping faults striking predominantly northeast or northwest with a pattern of motion consistent with north-south compression (Armbruster *et al.*, 1978). Surface expressions for many of these faults have been found. These faults are abruptly truncated by the Detachment at the lower boundary of the TSZ (17 km depth). The TSZ is also sharply bounded on the northeastern and southwestern sides (Figure 7), but there is no evidence that these boundaries correspond to faults. Thus, the active faulting, which is oriented at large angles to these vertical boundaries, probably continues beyond the seismicity. As a working hypothesis, we postulate that the TSZ is associated with a block of basement trapped in the decollement. Thus, the seismicity in the TSZ is not associated with an isolated region of high strain but is a result of the rheology of the basement rocks which are more brittle than the surrounding sedimentary rocks of the decollement.

The Indus fault system consists of a number of steeply dipping parallel faults that outcrop along the Indus valley north and south of Tarbela Dam and it is the most prominent seismic structure within the TSZ. Thus the seismicity indicates that the Indus fault system is active. However, the evidence for recent surface slip along these faults is not conclusive (Gross, 1971; Seeber, report in preparation).

B. Magnitude Distribution and b–values. Gutenburg and Richter (1944) proposed that the earthquake-magnitude distribution can be described by

$$\text{Log } N(M) = A - bM \qquad (1)$$

where N (M) is the number of earthquakes with magnitude M or greater (the cumulative number of earthquakes, A = Log N (0) is a function of the level of seismicity and of the length of the data-sample, and b is a constant, characteristic of the seismic area sampled.

The following three seismic data sets are chosen for the magnitude-distribution analysis:

1. Earthquakes from a volume within the Tarbela seismic zone (TSZ) 25 km long, 15 km wide and 20 km deep centered at the Tarbela site (Figures 7 and 9). This volume includes the Indus Valley fault zone, the source of the maximum credible earthquake for the Tarbela site (magnitude 6.5; Seeber *et al.*, 1974);

2. Earthquakes from a volume enclosing the central portion of the Indus-Kohistan seismic zone (IKSZ), the Himalayan Basement Thrust 70 km northeast of the Tarbela site (Figures 5 and 7);

3. Crustal earthquakes in an area 7 x 12 degrees centered on the Hazara arc which includes the Tarbela seismic network as well as the western Himalayas, the Pamirs and the eastern Hindu-Kush (depth 85 km; Figure 3).

While the data (1) and (2) are from the Tarbela seismic network (August 1973 — November 1976), the data in (3) are from the compendium of teleseismic data by Quittmeyer and Jacob (1979). To insure the completeness of this teleseismic data, only earthquakes from 1963 to 1975 are considered.

The b–values for these three data sets obtained from Utsu's (1971) maximum-likelihood method are presented in Tables 1, 2 and 3 and Figure 10. Table 4 summarizes the results.

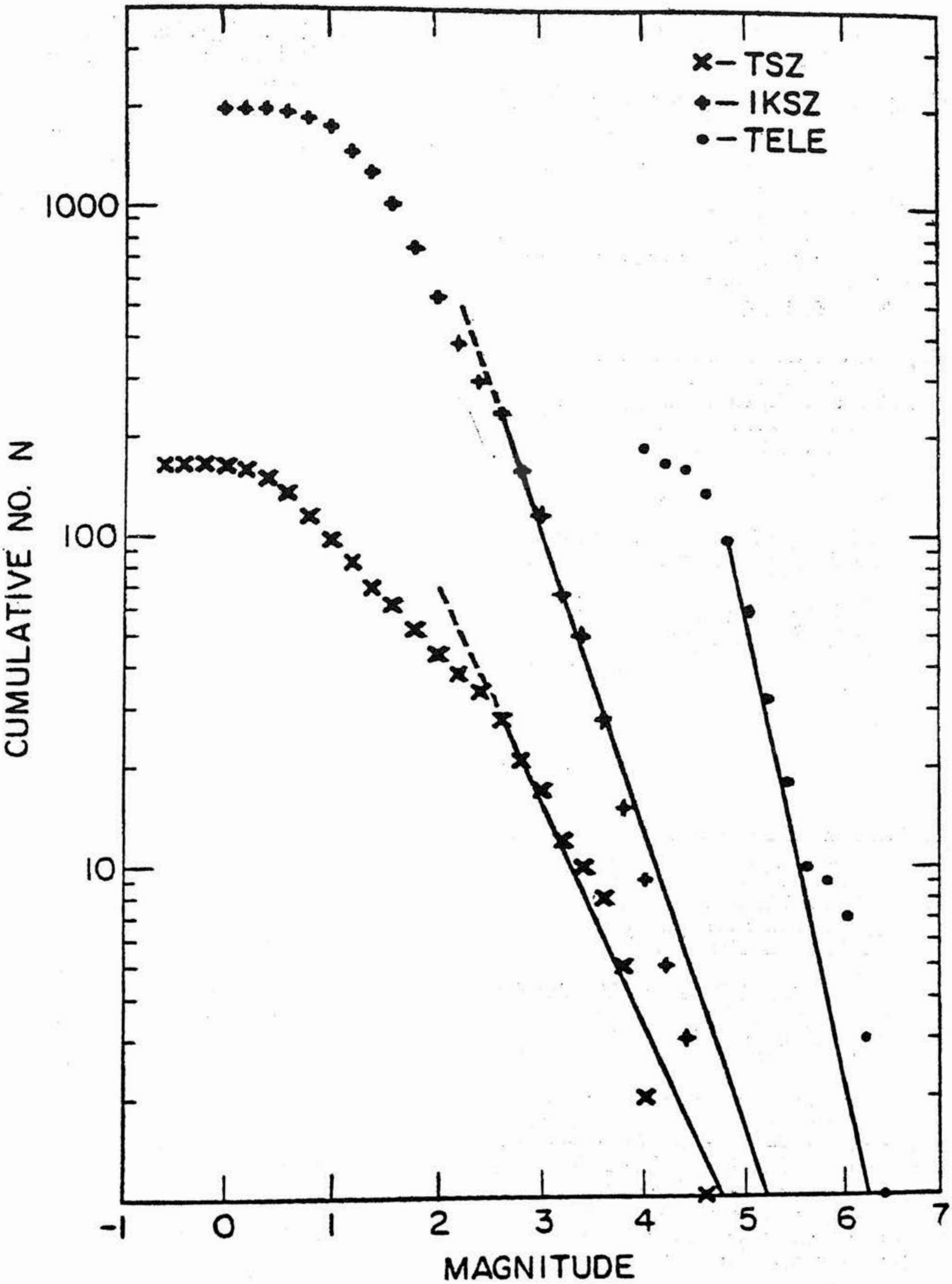

Fig. 10. Cumulative number of earthquakes (N) vs. magnitude (M) for 1) earthquakes in the Tarbela seismic zone (TSZ; X's) boxed in Figure 9; 2) earthquakes in the Indus-Kohistan seismic zone (IKSZ; crosses); 3) earthquakes with teleseismic crustal epicenters boxed in Figure 3 (dots). Note the difference in b-value (the slope of a straight-line fit of the data using Utsu's (1971) method) between the data sets. Also note the slope difference between the magnitude range above and below $M = 2.5$ for TSZ and IKSZ. We are confident that all earthquakes with $M > 0.6$ and $M > 1.6$, respectively, are being detected on these seismic zones. The significance of these differences is discussed in the text. See Tables 1 through 4.

TABLE 1

Magnitude in each	Range step	NO. OF EARTHQUAKES: In each step	NO. OF EARTHQUAKES: Cumulative	Average Magnitude	X	B VALUES: Uncorrected	B VALUES: Corrected for Finite Mag. step	B VALUES: ± Limits for 95% confidence	Correction for Finite Mag. step	Maximum Magnitude expected in Data sample	10^A (A in Eq. (1))
6.00	5.80	0	0	0.000	0.000	0.000	0.000	0.000	0.000	0.000	0.000
5.80	5.60	0	0	0.000	0 000	0.000	0.000	0.000	0.000	0.000	0.000
5.60	5.40	0	0	0.000	0.000	0.000	0.000	0.000	0.000	0.000	0.000
5.40	5 20	0	0	0.000	0.000	0.000	0.000	0.000	0.000	0.000	0.000
5.20	5.00	0	0	0.000	0.000	0.000	0.000	0.000	0.000	0.000	0.000
5.00	4.80	0	0	0.000	0.000	0.000	0.000	0.000	0.000	0.000	0.000
4.80	4 60	1	1	4.770	0.000	2.555	2 843	5.007	1.113	4.600	x x x x
4.60	4.40	0	1	4.770	0.000	1.174	1.202	2.301	1.024	4.400	194829.875
4.40	4.20	0	1	4.770	0 000	0 762	0.770	1.493	1.010	4.200	1709.169
4.20	4.00	1	2	4.428	1.505	1.016	1.034	1.408	1.018	4.291	27440.891
4.00	3 80	3	5	4.099	1.990	1.454	1 500	1.274	1.037	4.264	x x x x
3.80	3.60	3	8	3.939	1.021	1.279	1.316	0.887	1.029	4.296	438076.375
3.60	3.40	2	10	3.838	0 485	0 991	1.000	0.614	1.017	4.392	26688.673
3.40	3.20	2	12	3.743	0.396	0 801	0.810	0.453	1.011	4.533	4673.558
3.20	3 00	5	17	3.565	0.756	0.768	0.776	0.365	1.010	4.585	3627.184
3.00	2.80	4	21	3.436	0.459	0 683	0.689	0.292	1.000	4.720	1779.427
2.80	2 60	7	28	3.253	0.625	0.665	0.670	0.246	1.008	4.760	1546.140
2.60	2.40	6	34	3.120	0.422	0.603	0 607	0.203	1.006	4.923	973.857
2.40	2.20	4	38	3.034	0 242	0.521	0.523	0.166	1.005	5.220	538 001
2.20	2.00	6	44	2.902	0.318	0.482	0 484	0.142	1.004	5.399	407 885
2.20	2.00	6	44	2.902	0 318	0.459	0.461	0.125	1.004	5.521	351.594
2.00	1.80	8	52	2.745	0.363	0.446	0 447	0.111	1.003	5.609	321.959
1.60	1.40	8	70	2.450	0 264	0.414	0.415	0.097	1.003	5.847	266.690
1.40	1.20	13	83	2.264	0.370	0.408	0 409	0.088	1003	5.890	257.122
1.20	1 00	14	97	2.091	0.338	0.398	0.399	0.079	1.003	5.976	243.248
1.00	0.80	17	114	1.915	0.351	0.390	0 391	0.072	1.003	6.065	234.121
0.00	0.60	22	136	1.719	0 383	0.388	0.389	0.065	1.003	6.084	232.794 *
0.60	0.40	14	150	1.608	0.213	0.359	0 360	0.058	1.002	6.442	209.009
0.40	0 20	8	158	1.544	0.113	0.323	0.324	0.050	1.002	6.992	183.401
0.20	0.00	3	161	1.519	0.041	0.286	0.286	0.044	1.001	7.706	161.000
0.00	−0.20	2	153	1.500	0 027	0.256	0 256	0.039	1.001	8.448	144.886
−0.20	−0.40	0	163	1.500	0.000	0.229	0.229	0.035	1.001	9.268	132.025
−0.40	−0 60	0	163	1.500	0.000	0.207	0 207	0.032	1.001	10.087	122.459

Table 1. Magnitude-distribution and b-values (maximum-likelihood method; Utsu, 1971) for the seismicity from the TSZ boxed in Figure 9. The starred line corresponds to the magnitude limit for a complete data set; the other line corresponds with the flexure (see text). The results (TSZ) are plotted in Figure 10 and summarized in Table 4.

Results and Discussion. Had the magnitude distribution been uniform over the Hazara arc and surrounding regions, and had this distribution been described by eq. (1) only the constant A would have differed for each data set and the data points in Figure 10 would have fallen on three parallel lines. Instead, the points clearly indicate different slopes for each data set. Moreover, the magnitude distribution for the TSZ and IKSZ are non-linear since lines of different slop (b–value) fit the data in different magnitude ranges. In Table 4 the b–values are tabulated together with differences between these values. Most of the striking differences in the slope of the log N vs. M plots in Figure 10 are significant to better than 95%.

A non-linear magnitude distribution as in TSZ or in IKSZ is predicted for a data set that includes earthquakes from distinct seismic zones with different maximum-magnitude limits (Utsu, 1971). Non-linearity in the magnitude-distribution may also be the result of the fault-size distribution within a seismic zone (Caputo, 1977). The purpose here is not to discuss possible causes for the observed magnitude distribution, but only to provide a method to use such data for earthquake hazard evaluation.

The teleseismic data (TELE in Figue 10) are from a relatively large area that includes both the IKSZ and the TSZ (Figure 3). Much lower b–values are obtained for either of the network-data sets (TSZ and IKSZ in Figure 10) than for TELE. It is unlikely that the magnitude distribution in both TSZ and IKSZ are anomalous in the Hazara arc region since these seismic zones are prominent in the area sampled by TELE and

TABLE 2

Magnitude Range in each step		NO. OF EARTHQUAKES In each step	Cumulative	Average Magnitude	$\times$	B VALUES Uncorrected	Corrected for Finite Mag. step	± Limits for 95% confidence	Correction for Finite Mag. step	Maximum Magnitude expected in Data sample	10^A (A in Eq. (1))
6.00	5.80	0	0	0.000	0 000	0.000	0.000	0.000	0.000	0.000	0.000
5.80	5.60	0	0	0.000	0.000	0.000	0.000	0.000	0.000	0.000	0.000
5.60	5 40	0	0	0.000	0.000	0.000	0.000	0.000	0.000	0.000	0.000
5.40	5.20	0	0	0.000	0.000	0.000	0.000	0.000	0.000	0.000	0.000
5.20	5.00	0	0	0.000	0 000	0.000	0.000	0.000	0.000	0.000	0.000
5.00	4.80	0	0	0.000	0.000	0.000	0.000	0.000	0.000	0.000	0.000
4.80	4 60	0	0	0.000	0.000	0.000	0.000	0.000	0.000	0.000	0 000
4.60	4.40	3	3	4.473	2.386	5.936	9.240	6.717	1 557	4.452	0.000
4.40	4.20	2	5	4.373	1 109	2.515	2.790	2.204	1.109	4.451	x x x x
4.20	4.00	4	9	4.230	1.275	1 891	2.010	1.236	1.062	4.475	x x x x
4.00	3.80	6	15	4.085	1.109	1.524	1.586	0.771	1.041	4.542	x x x x
3.80	3.60	13	28	3.892	1.355	1.489	1.547	0.551	1 039	4.536	x x x x
3.60	3.40	22	50	3.697	1 259	1.461	1.516	0.405	1.037	4.521	x x x x
3.40	3.20	17	67	3.592	0.636	1 107	1.131	0.265	1.022	4.814	279158.906
3.20	3 00	48	115	3.398	1.173	1.092	1.115	0.200	1.021	4.848	254783.812
3.00	2.80	44	159	3.265	0.704	0.934	0.948	0 145	1.015	5.122	71738.391
2.80	2.60	78	237	3.083	0 867	0.900	0.913	0.115	1.014	5.202	55928.613
2.60	2.40	61	298	2.962	0.497	0 772	0.780	0.088	1.011	5.570	22244.383
2.40	2 20	90	388	2.808	0.573	0.714	0.721	0.071	1.009	5.792	14938.616
2.20	2.00	147	535	2.611	0.698	0.711	0.717	0 060	1.009	5.806	14528.009
2.00	1.80	213	748	2.406	0 728	0.717	0.724	0.051	1.009	5.772	15007.915
1.80	1.60	267	1015	2.215	0.663	0 706	0.712	0.043	1.009	5.820	14009.488
1.60	1 40	261	1276	2.066	0.497	0.853	0.657	0.036	1.008	6.125	10621.684
1.40	1.20	271	1547	1.929	0.418	0.596	0.600	0 030	1.006	6.516	8119.181
1.20	1.00	193	1740	1.834	0 255	0.521	0.523	0.024	1.005	7.195	5802.379
1.00	0.80	93	1833	1.787	0.113	0 440	0.441	0.020	1.003	8.192	4133.708
0.80	0 60	83	1916	1.742	0.096	0.380	0.381	0.017	1.003	9.209	3244.6?6
0.60	0.40	37	1953	1.719	0.042	0.329	0.330	0 015	1.002	10.377	2646.284
0.40	0.20	10	1963	1.712	0 011	0.287	0.288	0.013	1.001	11.649	2241.000
0.20	0.00	2	1965	1.711	0.002	0 254	0.254	0.011	1.001	12.957	1965.000
0.00	—0 20	0	1965	1.711	0.000	0.227	0.228	0.010	1.001	14.275	1769.534
—0.20	—0.40	0	1965	1.711	0.000	0.206	0.206	0 009	1.001	15.593	1625.522
—0.40	—0.60	0	1965	1.711	0 000	0.188	0.188	0.000	1.001	16.911	1515.362

Table 2. Magnitude-distribution and b-values for the seismicity in the IKSZ (Figure 7). See caption of Table 1. These results (IKSZ) are plotted in Figure 10 and summarized in Table 4.

TABLE 3

Magnitude Range in each step		NO. OF EARTHQUAKES In each step	Cumulative	Average Magnitude	$\times$	B VALUES Uncorrected	Corrected for Finite Mag. step	± Limits for 95% confidence	Correction for Finite Mag. step	Maximum Magnitude expected in Data sample	10^A (A in Eq. (1))
7 00	6.80	0	0	0.000	0.000	0.000	0.000	0.000	0.000	0.000	0 000
6.80	6.60	0	0	0.000	0.000	0.000	0.000	0.000	0.000	0.000	0 000
6.60	6.40	1	1	6.400	0.000	0 000	0.000	0.000	0.000	6.400	1.000
6 40	6.20	2	3	6.267	2.386	6.515	10.796	7.372	1.657	6.244	0.000
6.20	6.00	4	7	6.143	1.840	3.040	3.521	2 252	1.158	6.240	x x x x
6.00	5.80	2	9	6.067	0.546	1.629	1.704	1.064	1.046	6.360	x x x x
5 80	5.60	1	10	6.020	0.229	1.034	1 054	0.641	1.019	6.549	x x x x
5.60	5.40	8	18	5.767	1.276	1.184	1.214	0.547	1.025	6.434	x x x x
5.40	5.20	15	33	5.518	1.316	1.365	1.410	0 466	1.033	6.277	x x x x
5 20	5.00	26	59	5.300	1.262	1.448	1.501	0.369	1.037	6.180	x x x x
5.00	4.80	38	97	5.122	1.889	1.350	1 393	8.263	1.832	6.225	x x x x
4.80	4.80	38	135	4.990	0.718	1.113	1.137	8.188	1.022	6.474	x x x x
4 60	4.40	25	189	4.909	0.369	0.855	0.866	0 132	1.013	6.946	x x x x
4.40	4.20	7	167	4.881	0.093	0.637	0.642	0.987	1.007	7.663	82912.133
4 20	4.00	16	183	4.586	0.199	0 741	0.748	0.107	1.010	7.025	179405.266

Table 3. Magnitude-distribution and b-values for the teleseismic data from the area boxed in Figure 3 (March 1963 — April 1975; compiled by Quittmeyer and Jacob, 1979). See caption of Table 1. The results (TELE) are plotted in Figure 10 and summarized in Table 4.

TABLE 4

	A	B	C	D	E
	TSZ $M \geq 0.6^*$ N-136	TSZ $M \geq 2.6$ N=28	IKSZ $M \geq 1.6^*$ N=1015	IKSZ $M \geq 2.6$ N=237	TELE $M \geq 4.8^*$ N=97
Confidence 95%: Limit 80%:	b = 0.389 $\pm$ 0.065 = 0.389 $\pm$ 0.043	b = 0.670 $\pm$ 0.246 = 0.670 $\pm$ 0.162	b = 0.712 $\pm$ 0.043 = 0.712 $\pm$ 0.028	b = 0.913 $\pm$ 0.115 = 0.913 $\pm$ 0.076	b = 1.393 $\pm$ 0.269 = 1.393 $\pm$ 0.181
A	---	Δb = 0.281 =-0.030 (95%) = 0.028 (90%)	Δb = 0.323 = 0.215 (95%)	Δb = 0.524 = 0.344 (95%)	Δb = 1.004 = 0.670 (95%)
B		---	Δb Not Significant	Δb = 0.243 =-0.118 (95%) = 0.005 (80%)	Δb = 0.723 = 0.208 (15%)
C			---	Δb = 0.201 = 0.043 (95%)	Δb = 0.681 = 0.363 (95%)
D				---	Δb = 0.481 = 0.096 (95%)

Table 4. B-value difference chart. Each data-set (A through E) is characterized by the seismic zone (TSZ: Tarbela seismic zone; IKSZ: Indus Kohistan seismic zone; TELE: teleseismic data boxed in Figure 3) and by the low-magnitude limit. B-values (maximum likelihood; Utsu, 1971) with 95% and 80% confidence limits are listed with each data set. The values in the chart are the differences between the maximum likelihood b-values from the data-sets heading the corresponding row and column. Also listed are the smallest differences between b-values within the respective confidence limits (percentage as indicated). A negative value indicates that the confidence limits overlap by the given amount. The data sets are complete for magnitudes greater than starred values. M = magnitude; N = no. of earthquakes ir the indicated magnitude range. Note that the b-values are significantly different in the two seismic zones only 70 km apart (Figure 7), and within each seismic zone depending on the magnitude cut-off.

would contribute significantly to the magnitude distribution in this area. The different methods of determining magnitude used for the network and the teleseismic data are expected to introduce a bias. However, in order to eliminate the large difference in b-values between these data sets, very unreasonable magnitudes would have to be assigned to the local earthquakes (see Seeber and Armbruster, 1979, Appendix A).

The b-value for TELE is determined for magnitude $M \geq 4.8$ and no information regarding the magnitude-distribution in this range is available from either TSZ and IKSZ. Thus a flexure in the magnitude distribution plot at 4 M 5, similar to the one observed in both TSZ and IKSZ at M 2.6, can account for the large differences between the b-values of the teleseismic and of the network data.

C. Recurrence Time of Large Earthquakes and the Relative Level of Seismicity. The extrapolation of the TSZ data from low- to the high-magnitude assuming a linear magnitude-distribution yields erroneous results. For example, a magnitude 6.5 every 4.3 years would be expected on the Indus fault system near the Tarbela site (box in Figure 9) if the data from the TSZ for $M \geq 0.6$ is used assuming a linear distribution (Table 1). This is absurd considering the historic record (Figure 2).

The historic data could be reconciled with a linear distribution if the maximum credible magnitude for the TSZ is much smaller than $M = 6.5$ (Seeber *et al.*, 1974) and near the value of the maximum observed magnitude, $M = 5$. However, a very unusual maximum-magnitude to fault-length relationship would be required (Thatcher and Hanks, 1973).

Thus, we avoid a gross contradiction with historic seismicity or an incredibly low maximum magnitude by assuming that the magnitude distribution in the TSZ is not different from TELE in the magnitude range covered by the latter data. Specifically, we assume that the magnitude distribution in TSZ is represented by eq. (1), but in each specified magnitude range distinct values of the constants A and b apply. For $M < 4$ the parameters obtained directly from the TSZ apply. For $M < 5$ the parameters obtained for TELE apply instead. A flexure in the distribution occurs at $4 < M_F < 5$.

TABLE 5. Cumulative Number of Earthquakes at the Point of Flexure in TSZ (N_F)

TSZ: $M_C = 2.6$ $N_T = 28$ $N_C = 9.3$ $\text{Log } N_C = 0.97$ $b = 0.67 \pm 0.16$ (80%)

		$\text{Log } N_F = \text{Log } N_C - b(M_F - M_C)$	N_F
$M_F = 4.0$	$b = 0.83$	−0.19	0.64
	$b = 0.67$	0.03	1.08
	$b = 0.51$	0.26	1.80
$M_F = 4.5$	$b = 0.83$	−0.61	0.25
	$b = 0.67$	−0.30	0.50
	$b = 0.51$	0.00	1.00
$M_F = 5.0$	$b = 0.83$	−1.02	0.09
	$b = 0.67$	−0.64	0.23
	$b = 0.51$	−0.25	0.56

Each linear portion of the magnitude-distribution satisfies eq. (1), and for any two magnitudes M_A and M_B within the same segment

$$\text{Log } N(M_A) = \text{Log } N(M_B) - b\,(M_A - M_B) \quad (2)$$

The b–values appropriate for each segment are given in Table 4. The results are in Table 7 through 9. Table 10 is a summary of the results. The symbol used are:

N_T = Total number of earthquakes in the data set.

M_C = Low-magnitude cutoff for the data set.

N_C = Number of earthquakes with $M \geq M_C$ per year.

M_F = Magnitude at the flecture in the distribution plot.

N_F = Number of earthquakes with $M \geq M_F$ per year.

M_M = 6.5, maximum credible magnitude within the TSZ.

N_M = Number of maximum credible earthquakes per year = (Recurrence time)$^{-1}$.

M_P = Maximum probable earthquake in 50 years.

R_T = Recurrence time, years.

TABLE 6. Cumulative Number of Earthquakes at the Point of Flexure in TELE (N_F)

TELE: M_C = $N_T = 97$ $N_C = 8.08$ $\text{Log } N_C = 0.91$ $b = 1.39 \pm 0.18$ (80%)

		$\text{Log } N_F = \text{Log } N_C - b(M_F - M_C)$	N_F
$M_F = 4.0$	b = 1.57	2.17	148
	b = 1.39	2.02	105
	b = 1.21	1.88	76
$M_F = 4.5$	b = 1.57	1.38	24
	b = 1.39	1.33	21
	b = 1.21	1.27	19
$M_F = 5.0$	b = 1.57	0.60	4.0
	b = 1.39	0.63	4.3
	b = 1.21	0.67	4.7

Symbols and Procedures: see Table 5

TABLE 7

Ratio of the seismic activity in the source area of TSZ boxed in Figure 9 = 375 km² to the average seismic activity in the source area of TELE boxed in Figure 3 = 825,000 km². (The difference in the depth range of the two data sets is ignored).

N_F of TSZ from Table 5; N_F of TELE from Table 6
area TELE/area TSZ = 2,200

		N_F (TSZ)/N_F (TELE)	N_F (TSZ)/N_F (TELE) x 2,200 = seismicity of TSZ/seismicity in TELE
$M_F = 4.0$	Maximum	1/231	9.5
	Most Likely	1/97	23
	Minimum	1/42	52
$M_F = 4.5$	Maximum	1/96	23
	Most Likely	1/42	52
	Minimum	1/19	116
$M_F = 5.0$	Maximum	1/52	42
	Most Likely	1/18	122
	Minimum	177.1	310

Symbols and Procedures: see Table 5

The assumption that eq. (1) applies to discrete segments of the magnitude distribution implies that the flexures occur at a point rather than over a finite range of magnitude. This convenient, but probably incorrect (Utsu, 1971) approximation effects the results somewhat, but only in the conservative direction.

The frequency of earthquakes with magnitude $M \leq M_F$ in TSZ is calculated from the TSZ data for $M \geq 2.6$ (Table 5). Then, the recurrence-rate for the maximum credible earthquake, and other statistical parameters are computed from the b-value of TELE (Tables 6 through 9). The results are summarized in Table 10.

There are at least three causes for uncertainties in the results listed in Table 10: the b–values; the magnitude at the flexure in the distribution; and the assumption of a non-linear magnitude-distribution. The calculations leading to Tables 5 through 9 are carried out for the most likely values as well as for the extreme values leading to the highest and lowest estimate of seismic hazard. These extreme b–values are taken in the 80% confidence limits (Aki, 1965); the extreme values for M_F are taken as 4.0 and 5.0 since this magnitude range is not well covered by either TSZ and TELE (Tables 1 and 3) and a flexure is possible anywhere within it. Since most of the uncertainty in the results is due to the uncertainty in the b-values, the final results can be considered close to an 80% level of confidence.

TABLE 8. Recurrence Time for the Maximum Credible Earthquake, $M_M = 6.5$

N_F from TSZ (Table 5); b = 1.39 ± 0.18 (80%) from TELE (Table 4)

		$\text{Log } N_M = \text{Log } N_F - (M_M - M_F)$	N_M	$R_T = N_M^{-1}$ yrs.
$M_F = 4.0$	b = 1.57	−4.11	$7.7. \times 10^{-5}$	13,031
$N_F = 0.64$	b = 1.39	−3.66	2.2×10^{-4}	4,624
= minimum value	b = 1.21	−3.21	6.1×10^{-4}	1,641
$M_F = 4.5$	b = 1.57	−3.44	3.6×10^{-4}	2,754
$N_F = 0.50$	b = 1.39	−3.08	8.3×10^{-4}	1,202
= maximum likelihood value	b = 1.21	−2.72	1.9×10^{-3}	525
$M_F = 5.0$	b = 1.57	−2.60	2.5×10^{-3}	403
$N_F = 0.56$	b = 1.39	−2.33	4.6×10^{-3}	216
= maximum value	b = 1.21	−2.06	8.6×10^{-3}	116

Symbols and Procedures: see Table 5

TABLE 9

TSZ: Maximum Probable Earthquake in 50 years (M_P)

N_F from TSZ (Table 5); b = 1.39 ± 0.18 (80%) from TELE

$$\text{Log } (1) = \text{Log } (N_F \times 50) - b\,(M_P - M_F)$$

$$M_P = \frac{1.70 + \text{Log } N_F + b\,M_F}{b}$$

		M_P
$M_F = 4.0$; $N_F = 0.64$ (= minimum value)	b = 1.57	5.0
	b = 1.39	5.1
	b = 1.21	5.2
$M_F = 4.5$; $N_F = 0.50$ (= maximum likelihood value)	b = 1.57	5.4
	b = 1.39	5.5
	b = 1.21	5.7
$M_F = 5.0$; $N_F = 0.56$ (= maximum value)	b = 1.57	5.9
	b = 1.39	6.0
	b = 1.21	6.2

Symbols and Procedures: see Table 5

TABLE 10. Summary of Results

	Maximum probable earthquake on the Indus fault zone at the Tarbela site during a 50 year lifetime of the dam	Recurrence time of maximum credible earthquake (M = 6.5) on the Indus fault zone at the Tarbela site	Probability of the maximum credible earthquake M = 6.5) occurring during a 50 year lifetime	Factor by which the seismic activity in the Indus fault zone (boxed in Fig. 9) is higher than the average activity over the Hazara arc and surrounding region (boxed in Fig. 3)
Most favourable likely value (~ 80%)	5.0	13,000 years	1/260	10
Most likely value	5.5	1,200 years	1/24	50
Least favourable likely value (~ 80%)	6.2	116 years	1/2.4	300

CONCLUSIONS

Of the tectonic environments associated with seismicity that is potentially hazardous at the Tarbela dam site, the Tarbela seismic zone (TSZ), within the sedimentary wedge, is of greatest concern. The maximum credible event, a M = 6.5 earthquake associated with surface rupture, a displacement of more than a meter, and a maximum acceleration of 0.5g at the site (Seeber *et al.,* 1974), is likely to occur every 1200 years, which is equivalent to a probability of 1/24 for this event to occur during a 50 year lifetime of the dam. The most likely maximum probable event during a 50 year period is a M = 5.5 earthquake. The effects at the site from this event will depend on the location of the associated rupture in the volume boxed in Figure 9. A surface rupture from this event is less likely than for the maximum credible event, but it is conceivable. Similarly, a high maximum acceleration from this event (0.5g) is also possible, while the expected duration would be considerably shorter than the duration of the maximum credible event.

The potential for damage at the Tarbela site associated with the Detachment is subject to large uncertainties. The Detachment provides the largest fault surface that could rupture in a single event in the entire Hazara arc region, from the Salt Range to the Basement Thrust. The effects from a major earthquake in this area can be as devastating as the effects from the great Indian earthquakes. However, the Detachment in the Hazara arc, unlike the Detachment in the central portion of the Himalayan front, may not be associated with stress accumulation leading to great earthquakes because the thick salt layer that is associated with the Detachment in the Hazara arc may deform aseismically by creep. Historic data are not in conflict with this hypothesis since the only reported event which could be associated with a major Detachment earthquake is the 25 AD Taxila earthquake (Ambraseys *et al.,* 1975). This event could also have occurred on other large faults in the Taxila area such as the HLSZ (Figure 7).

The uncertainty regarding the seismic hazard associated with the Detachment concerns a large area of Pakistan which is now being rapidly developed including the Tarbela site, Islamabad, Rawalpindi and the Potwar. We urge a program of studies in this area to reduce this uncertainty, such as repeated precise geodetic measurements.

The maximum credible earthquake on the IKSZ is small considering the length of this structure. Thus, the estimated hazard from the IKSZ is localized near this fault zone where high intensity can be expected as demonstrated by the 1974 Pattan event.

The HLSZ is closer to the Tarbela site than the IKSZ and has been much less active during the period of network operations (Figure 7). Until the tectonic significance of the HLSZ is better understood and more is known on its predominant mode of slip, this basement strike-slip fault, deeply buried under the Tarbela site, should be conservatively considered a possible source of large earthquakes. The worse effects from these events are expected along the northeastern border of the Peshawar basin, including the Tarbela site.

Acknowledgements: The data that provides the basis for this work could not have been collected and analyzed without the dedicated effort of the scientists and technicians from WAPDA/TAMS which have been an integral part of the Seismic Project at Tarbela Dam. We are particularly grateful to Mr. Saggiad Hussain. The authors are grateful to WAPDA/TAMS for their continuing support. This work was also partially supported by NSF (EAR 77-15187) and by the USGS (14-08-0001-16749). K. Jacob, R. Quittmeyer, and Y. Aggarwal reviewed the paper and offered many helpful suggestions. Lynn Zappa typed the manuscript and Kazuko Nagao drafted the figures.

REFERENCES

Aki, K., 1965. Maximum likelihood estimate of b in the formula Log N = a-bM and its confidence limits, *Bull. Earthquake Res. Inst.*, 43, 237-239.

Ambraseys, N., G. Lensen, and A. Moinfar, 1975. The Pattan earthquake of 28 December 1974, UNESCO Report RP/1975-76/2.222.3, Paris.

Armbruster, J., L. Seeber, and K.H. Jacob, 1978. The northern termination of the Himalayan mountain front: active tectonics from microearthquakes, *Jour. Geophys. Res.*, 83, n. B1, 269-282.

Auden, J.B., 1970. Report on the possible ages of earth movements in the vicinity of the Tarbela dam, West Pakistan, Report to TAMS.

Bally, A.W., 1975. A geodynamic scenario for hydrocarbon occurrences, in *Global Tectonics and Petroleum Occurrences,* also in *Proceedings 9th World Petroleum Congress, Tokyo, 2, Geology.*

Borchert, H., and R.O. Muir, 1964. *Salt Deposits,* D. Van Nostrand Co., London.

Bordet, P., M. Colchen, D. Krummenacher, P. LeFort, R. Mouterde, and J.M. Remy, 1971. Recherches geologiques dans l'Himalaya du Nepal, region de la Thakkhola, *Ed. C.N.R.S.*, Paris, 270 p.

Caputo, M., 1977. A mechanical model for the statistics of earthquake magnitude moment and fault distribution, *Bull. Seismol. Soc. Amer.*, 67.

Davies, J.N., and L. House, 1979. Aleutian subduction zone seismicity, volcano-trench separation, and their relation to great thrust-type earthquakes, *Jour. Geophys. Res.*, 84, 4583-4591.

Fitch, T.J., 1972. Plate convergence transcurrent faults, and internal deformation adjacent to Southeast Asia and the western Pacific, *Jour. Geophys. Res.*, 77, 4432-4460.

Gansser, A., 1964. *Geology of the Himalayas,* Inter-Science Publishers, John Wiley and Sons, London.

Gron, J. TAMS Inter-office correspondence IC-SF(GBO)/593, dated 1/3/79.

Gumper, F.J., and C. Scholz, 1971. Microseismicity and tectonics of the Nevada seismic zone, *Bull. Seismol. Soc. Amer.*, 61, 1413-1432.

Gutenberg, B., and C.F. Richter, 1944. Frequency of earthquakes in California, *Bull. Seismol. Soc. Amer.*, 34, 185-188.

Gutenberg, B., and C.F. Richter, 1954. *Seismicity of the Earth and Associated Phenomena,* Princeton University Press, Princeton, New Jersey, 273 p.

Hasegawa, A., N. Umino, and A. Takagi, 1978. Double planed structure of the deep seismic zone in the northeastern Japan Arc, *Tectonophysics,* 47, 43 58.

Isacks, B.L., and M. Barazangi, 1977. Geometry of Benioff zones: Lateral segmentation and downwards bending of the subducted lithosphere, Maurice Ewing Series 1, Talwani and Pitman (eds.).

Jacob, K.H., 1974. A magniture scale for the Tarbela seismic network, L-DGO Report to TAMS/WAPDA.

LeFort, P., 1975. Himalayas: The collided range. Present knowledge of the continental arc, *Amer. Jour. Sci.* 275A, 1-44.

Lehner, E., 1944. The age of the Punjab Saline Series: Possible reconciliation of the opposing views, in *Proceedings of the National Academy of Sciences, India.*

Mathur, L.P., and P. Evans (editors), 1964. Oil in India, *22nd Inter. Geol. Congress.*

Molnar, P., and P. Tapponnier, 1975. Cenozoic tectonics of Asia: Effects of a continental collision, *Science,* 189, 419-426.

Molnar, P., W.P. Chen, T.J. Fitch, P. Tapponnier, W.E.K Warsi, and F.T. Wu, 1977. Structure and tectonics of the Himalaya: A brief summary of relevant geophysical observations. *Proc. C.N.R.S Symp. Geol. Ecol.,* Himalayas, Paris, December 1976.

Oxburgh, E.R., 1972. Flake tectonics and continental collision, *Nature,* 239, 202-204.

Pennington, W., 1979a. A summary of field and seismic observations of the Pattan earthquake — 28 December 1974, in *Geodynamics of Pakistan,* A. Farah and K. DeJong (eds.).

Pennington, W., 1979b. The Pattan (Pakistan) earthquake of 28 December 1974: Seismologic observations and tectonic implication, Dept. Geol. and Geophys., Univ. Wisconssin, Madison (preprint).

Powell, C.McA., and P.J. Conaghan, 1973. Plate tectonics and the Himalayas, *Earth Planet. Sci. Lett.,* 20, 1-12.

Quittmeyer, R.C., and K.H. Jacob, 1979. Historical and modern seismicity in Pakistan, Afghanistan, Northwest India, and Southeast Iran, *Bull. Seismol. Soc. Amer.,* 69, 773-823.

Quittmeyer, R.C., A. Farah, and K.H. Jacob, 1979. The seismicity of Pakistan and its relation to surface faults, in *Geodynamics of Pakistan,* A. Farah and K. DeJong (eds.), Quetta, 271-284.

Richter, C.F., 1958. *Elementary Seismology,* W.H. Freeman and Company, San Francisco and London, 768 p.

Scholz, C.H., L.R. Sykes, and Y.P. Aggarwal, 1973. Earthquake prediction: A physical basis, *Science,* 181, 803.

Seeber, L., 1974. Vibrations, structural responses, and seismic events associated with the first impounding of the Tarbela reservoir, Report for Special Consultants Meeting, Sept./Oct. 1974, TAMS/T.D.P. Folio IM-P-33.

Seeber, L., K.H. Jacob, and J. Armbruster, 1974. Tectonics, design earthquakes, and seismic risk for the Tarbela dam project, Pakistan, L-DGO Report to TAMS/ WAPDA.

Seeber, L., and K.H. Jacob, 1977. Microearthquake survey of northern Pakistan: Preliminary results and tectonic implications, *Proc. C.N.R.S. Colloquium Geology and Ecology of the Himalayas,* Paris, December 1976.

Seeber, L., and J. Armbruster, 1979a. Seismicity of the Hazara arc in northern Pakistan: Decollement vs. basement faulting, in *Geodynamics of Pakistan,* A. Farah and K. DeJong (eds.), Spec. Pubu. GSP, Quetta.

Seeber, L., and J. Armbruster, 1979b. Seismic hazard at the Tarbela dam site from a model of the active tectonics and earthquake magnitude distribution, Report to WAPDA/TAMS, June 1979.

Seeber, L., R. Quittmeyer, and J. Armbruster, 1979. Seismotectonics of Pakistan: A review of results from network data and implications for the central Himalaya, in *Structural Geology of the Himalaya,* P.S. Saklani (ed.), 361-392.

Seeber, L., J. Armbruster, and R. Quittmeyer, 1980. Seismicity and continental subduction in the H'malayan arc, Interunion Commission on Geodynamics, Working Group 6 Volume.

TAMS, January, 1969. Tarbela Dam: Summary of proposed project.

Thatcher, W., and T.C. Hanks, 1973. Source parameters of southern California earthquakes, *Jour. Geophys. Res.,* 78, 8547-8576.

Toksoz, M.N., and P. Bird, 1977. Tectonophysics of the continuing Himalayan orogeny, *Proc. C.N.R.S. Symposium Geol. Ecol. Himalayas,* Paris, December 1976.

Utsu, T., 1971. Aftershocks and earthquake statistics, III., *Jour. Fac. Sci. Hokkaido Univ. Ser. VII, Geophysics, III,* 379-441.

Wadia, D.N., 1961. *Geology of India,* MacMillan III Edition.